# Comprehensive microanalytical study of welding aerosols with x-ray and Raman based methods

**A. Worobiec,[1]\* E. A. Stefaniak,[1,3] S. Kiro,[2] M. Oprya,[2] A. Bekshaev,[4] Z. Spolnik,[1] S. S. Potgieter-Vermaak,[1] A. Ennan[2] and R. Van Grieken[1]**

[1] University of Antwerp, Department of Chemistry, Universiteitsplein 1, B-2610 Antwerp, Belgium
[2] Physico-Chemical Institute for the Environmental and Human Protection, National Academy of Science of Ukraine, Preobrazhenska 3, 65026, Odessa, Ukraine
[3] Catholic University of Lublin, Department of Chemistry, Al. Kraśnicka 102, 20-718 Lublin, Poland
[4] I.I. Mechnikov National University, Department of Physics, Dvoryanska 2, 65026 Odessa, Ukraine

A comprehensive analysis of individual welding fume particles of different size fraction has been performed by applying of an innovative combination of the energy-dispersive x-ray fluorescence spectroscopy (EDXRF), micro-Raman spectroscopy (MRS) and electron probe microanalysis (EPMA). Owing to this set of analytical techniques, a systematic study of the chemical composition along with the size, morphology and structure parameters of the collected welding particles was performed. The results show distinct interdependencies between the particles' elemental composition and their sizes and structures, which are consistent with commonly assumed mechanisms of their formation and evolution. In particular, interactions between the particles of fine and coarse fractions as well as regularities in distribution of the most toxic welding fume components (Mn and its oxides) have been observed. Copyright © 2007 John Wiley & Sons, Ltd.

## INTRODUCTION

Arc welding technologies are widely used in many industries. Along with obvious technical advantages, they pose substantial hazards to the human health and the environment. In particular, the welding fume (welding aerosol) contains respirable particles with high content of chemicals that cause adverse effects after inhalation. In the whole world, about 0.5–2% of industrial workers of different professions (about 3.5 million people) are affected by welding waste.[1,2] Therefore, the harmful influence of welding fumes on human health and the possible ways for its neutralization are subjects of intensive research activity.[1–5]

Recent studies[5–10] have shown that harmful effects of welding fumes are mainly stipulated by chemicals constituting the fume particles and gases. The most toxic agents essentially presented in wide range of welding technologies are heavy metals, mainly nickel, chromium and manganese, and their compounds. However, the harmful influence of these agents strongly depends on their chemical form and on the size and morphology of aerosol particles they are carried in. For example, airborne particles of several micrometers in diameter and greater, are generally deposited in the walls of human airway and do not reach the lungs;[6,8] besides, such particles can be efficiently trapped by usual filtering systems. On the contrary, particles smaller than 0.1 μm are inhaled and deposited in the lungs, constituting thus the most harmful part of welding aerosol. The intermediate fraction (0.1–1 μm) can be exhaled and only a minor part of them really affects the human organism.[8] In the latter case, the probability for toxic substances to penetrate into the body is essentially dictated by morphological peculiarities of individual particles or aggregates. On the other hand, physical properties and structure of the welding aerosol particles essentially affect the efficiency of air-cleaning methods used in various welding technologies. An important aspect is that during the transportation of the welding fumes to the filtering system, the evolution of the aerosol particles continues. As a result, the particle components can change their chemical state; the structure of the particles themselves can be modified and agglomerates can be formed. In this process, toxic agents can be redistributed between different fractions and types of particles. Such processes must also be taken into account upon the choice of cleaning methods and in design of filtering and ventilation equipment.

In view of the evident importance of the problem, a lot of efforts have been made to determine the chemical composition[7,9,10] as well as size and structural parameters of the welding fume particles.[6,8,9,11] Employing the most efficient and informative analytical techniques, including x-ray diffraction and spectrometry, electron- and laser-probe microanalysis, atomic emission and absorption optical spectroscopy, neutron activation analysis, mass spectrometry, etc., have enabled to achieve a rather full knowledge on the bulk chemical composition and microstructure speciation of welding fumes at various welding regimes and technologies.[7] Various types of impactors and particle counters in conjunction with optical and electron microscopy

\*Correspondence to: A. Worobiec, University of Antwerp, Department of Chemistry, Universiteitsplein 1, B-2610 Antwerp, Belgium. E-mail: anna.worobiec@ua.ac.be

yield valuable information on the fume particles' shapes, external structures and size distributions.[7,12] Considering the above, in case of the welding fumes, particle size distribution and morphology must be investigated inseparably from its chemical composition, because of their interrelationship and mutual dependencies

This paper presents an attempt of solving this problem for a selected but rather typical and widespread situation of welding with standard mild-steel rutile-coating electrode. After collecting the fume samples with an impactor, we determined bulk chemical content of welding aerosols as well as the elemental compositions of individual fume particles of different sizes and morphologies. During this study, three micro- and trace analysis techniques were applied. Electron probe microanalysis (EPMA) with energy-dispersive x-ray detection was employed for the characterisation of individual particles, because it allows characterising large numbers of particles in a fast, automated way and can give detailed information about their elemental composition, size distribution and morphology. Special attention was paid to the microanalysis of individual particles by EPMA in conjunction with micro-Raman spectrometry (MRS). This approach creates a possibility for further studies of the particles' molecular composition. Bulk trace analysis was performed by the energy-dispersive x-ray fluorescence (EDXRF) method.

The results presented below show peculiarities of the distribution of the chemical constituents of the welding fumes over various size fractions. They reveal correlations between the particle composition and its dimensional and morphological parameters, which comply with the conventional mechanisms of the welding fume formation.[13]

## EXPERIMENTAL

In order to control the welding conditions and provide a stable welding fume production during several minutes, a laboratory set-up as shown in Fig. 1 was used. A standard mild-steel electrode with rutile coating (E6013) and a 4 mm wire diameter was placed at 45° to the mild-steel plane substrate. The general composition of the electrode includes, as basic elements, Fe, Mn, Si, Na, K, Ti, Al, Mg, O, C (concentration 0.5–10%) and, as impurities, Ca, Cr, Cu, Zn, Pb, S, Cl, F (concentration below 0.5%).[10] An automated wire-feeding unit maintained the constant wire feed speed of 4.3 mm/s with a welding travel speed of 3.3 mm/s. The welding current density varied within the range 12.7–17.5 A/mm². The air was pulled up vertically through the box by the exhauster, with a delivery of 1800 l/min and a depression of 7.0 kPa, and entered the gas-collecting system through the outlet situated at 30 cm above the arc plume, which enabled collection of the whole fume.

For bulk analysis by the EDXRF technique, the fume particles were collected by a Stacked Filter Unit on Nuclepore filters. For spectroscopic analyses of individual particles (low-Z element EPMA and MRS), samples were collected on non-organic substrates (Si, Ag) by a cascade Berner impactor with a low-volume vacuum pump (30 l/min). This way of collection allows a size segregation of the particles according
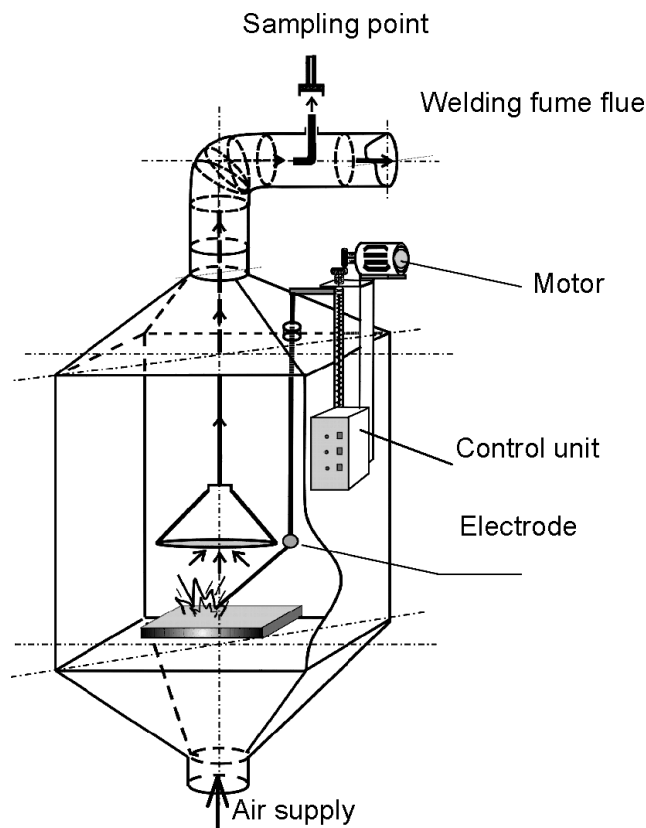


**Figure 1.** The experimental set up.

to their aerodynamic diameters.[14] The particle size ranges (cut-off diameters) for the used stages, 3, 4, 5, 6, 7 and 8, of the Berner cascade impactor were equal to 0.25, 0.5, 1, 2, 4 and 8 μm, respectively. The impactor was connected to the gas-collecting pipe at the distance 2 m from the welding plume. Since the mass concentration of particulate matter in the pipe (0.35–1 g/m³) exceeds the value necessary for a proper performance of the impactor (0.02 g/m³), the collected welding fume samples were diluted by an injection-type diluter in a proportion 1 : 100. The sampling time was optimized in order to obtain the best loading of particles in the impactor spots and varied from a few seconds for stages 3 and 4 to approximately 100 s for stages 7 and 8.

Low-Z EPMA (Z ≥ 6) was carried out on a JEOL 733 (Tokyo, Japan) electron probe micro-analyser equipped with a super-atmospheric thin-window OXFORD energy-dispersive x-ray detector. Particles from impactor stages 3 and 4 were collected on Si substrate and therefore analysed manually (100 particles at each stage). Particles from stages 5, 6, 7 and 8 were deposited on Ag foil and analysed in an automated mode using the homemade software (400 objects at each stage). To achieve optimal experimental conditions, such as low background levels in the spectra and high sensitivity for light element analysis, an accelerating voltage of 10 kV and a beam current of 1 nA were applied.[15] Automatic and manual measurements were carried out in the spot mode.

The characteristic x-ray spectra from the low-Z element EPMA were evaluated by non-linear least-squares fitting, using the AXIL code.[16] The semi-quantitative elemental composition of the particles was calculated with

an iterative approximation method based on Monte Carlo simulations.[15,17,18] The obtained data set was used for the further particle classification by means of hierarchical cluster analysis performed with the Integrated Data Analysis System program.[19] The clustering was done only on the basis of the chemical composition of the aerosol particles and not on the morphological information. The separate samples were clustered independently. The visual/manual analysis with respect to the changes in the morphology of the individual particles in the different particle fractions was performed on JEOL JSM 6300 scanning electron microscope (JEOL, Tokyo, Japan). Analysis of the molecular and phase composition of particles was performed by means of MRS (Renishaw inVia Reflex, Wotton under Edge, UK) coupled with a Peltier cooled CCD detector (576 × 288 pixels) and equipped with two lasers of 514 nm and 785 nm wavelengths. Calibration was done using the 520.5 cm$^{-1}$ band of a silicon wafer. Data acquisition was carried out with the Spectracalc software package GRAMS (Galactic Industries, Salem, NH, USA).

Determination of elements in the whole sample (bulk analysis) was done by EDXRF (Tracor Spectrace 5000) equipped with a low-power Rh-anode x-ray tube (17.5 W). The characteristic x-ray radiation was detected by a Si(Li) detector. For determining high-Z elements (starting from K), an accelerating voltage of 35 kV and current of 0.35 mA were used. The acquisition time was set at 10 000 s. Low-Z elements (from Al to Cl) were measured at 10 kV and 0.35 mA with an acquisition time of 4000 s. The measured intensities were converted into elemental concentrations by the application of the AXIL software.[16] The results represent normalized surface concentrations of elements collected on a filter ($\mu g/cm^2$).

## RESULTS AND DISCUSSION

### Elemental bulk concentration

Results of the bulk sample analyses performed by the EDXRF method (Table 1) show the general composition of the investigated particulate matter at different welding regimes specified by the arc current densities. Despite the known increase of fume emission with growing arc current,[10] changes in the fume elemental compositions are inessential or show no explicit trends. Therefore, only one welding regime

**Table 1.** Bulk elemental composition of welding aerosol at different arc current regimes

| Welding arc current density, A/mm$^2$ | Concentrations of most abundant elements in samples, µg/cm$^2$ | | | | | | |
|---|---|---|---|---|---|---|---|
| | Fe | Ca | K | Mn | Si | Ti | Al |
| 12.7 | 8.76 | 0.09 | 0.49 | 1.1 | 0.81 | 0.08 | 0.26 |
| 14.3 | 8.61 | 0.09 | 0.60 | 1.15 | 0.94 | 0.19 | 0.17 |
| 15.9 | 8.05 | 0.04 | 0.90 | 1.24 | 1.27 | 0.23 | 0.19 |
| 17.5 | 8.45 | 0.03 | 0.71 | 1.14 | 1.18 | 0.26 | 0.19 |

with arc current density 14.3 A/mm$^2$ was selected for more comprehensive investigations at the single particle level.

The results of a low-Z element EPMA of separate particle fractions are given in Table 2. The presented data were obtained by averaging the measured elemental composition over all particles found in each size fraction. The most significant differences were observed when comparing the fine (diameters < 0.5 µm) and coarse (> 1 µm) size fractions. Fraction with cut-off diameter 0.25 µm is characterized by a relatively higher content of O, K, Na, Mg and a low concentration of Fe and Mn. Within the coarse fractions, the contents of practically all the most abundant elements (Fe, Mn, K, Si, Mg, Na, O, C) do not depend on particle size. Elements such as Cr, V, Ti, Al, for which concentrations increase with the particle size, are exceptional. The observed variability of the chemical composition is apparently caused by differences in the mechanisms responsible for formation of fine and coarse particles.

In accordance with the commonly used notion,[6,12] fine fractions are composed by particles of the so-called nucleation mode and their agglomerates. They are formed by the typical 'condensation' mechanism.[10,21] It occurs when high-temperature vapours of the welded metal and electrode components under the action of plasma flows are pushed out of the arc column to the ambient air with a lower temperature. There, the consecutive condensation of individual elements takes place, in accordance with the degree of their supersaturation and possible vapour-phase reactions; simultaneously, some condensation products are oxidized. The soot particles formed after combustion of the

**Table 2.** Mean elemental composition of different fractions of the welding fume particles (last row represents the normalized bulk composition of the total welding fume mass at 14.3 A/mm$^2$, Table 1)

| Fraction cut-off diameter, µm | Percentage of elements in fraction, % | | | | | | | | | | | | | |
|---|---|---|---|---|---|---|---|---|---|---|---|---|---|---|
| | Fe | Mn | Cr | V | Ti | Ca | K | Si | Al | Mg | Na | O | N | C |
| 0.25 | 11 | 3.4 | — | — | — | 0.8 | 4.9 | 7.6 | — | 3.5 | 7.4 | 53 | — | 8.4 |
| 0.5 | 15 | 2.9 | — | — | 0.7 | — | 2.7 | 6.2 | — | 0.6 | 1.4 | 65 | — | 5.2 |
| 1 | 36 | 4.9 | — | — | 1.1 | — | 2.5 | 6.5 | — | 1.1 | 1.2 | 38 | — | 7.7 |
| 2 | 40 | 4.8 | — | — | 1.4 | 1.1 | 2.3 | 6.0 | 0.5 | 1.5 | 1.0 | 33 | 0.6 | 7.7 |
| 4 | 40 | 5.2 | — | — | 2.1 | 1.8 | 2.5 | 6.0 | 0.8 | 1.4 | 0.9 | 32 | 1.0 | 6.9 |
| 8 | 38 | 4.9 | 0.5 | 0.7 | 2.7 | 0.7 | 2.0 | 5.0 | 0.9 | 1.5 | 0.7 | 32 | 1.2 | 8.8 |
| Particulate matter in total | 40 | 5.3 | — | — | 0.9 | 0.4 | 2.7 | 4.4 | 0.8 | 0.5* | 3.0* | 33* | — | — |

* Data from Ref. 20.

cellulose and wood flour (gas-producing components of the electrode coating) play the role of condensation nuclei. Therefore, fine particles are expected to have a multi-layer structure typical for consecutive condensation of a high-temperature multi-component vapour.[10] The carbon core is surrounded by the oxides of Fe, Mn and Mg, which are condensed first; above this layer, compounds of K, Na and Si can be deposited. However, because of high-temperature gradients in the condensation zone, particles of nucleation mode generally cannot grow above 0.5 µm.[10]

The relatively large particles of the coarse fractions (usually referred to as microspatter[6,22]) are formed by a different mechanism, from ejection and explosion of liquid droplets consisting predominantly of molten welded metal and electrode components.[10,12] This is reflected in the qualitative difference of their elemental composition (e.g. Table 2). In particular, the microspatter mechanism is consistent with the high content of Fe in coarse particles and with a decrease of the Mn/Fe ratio to 0.05–0.13, which is characteristic for the slag melt. The value of Mn/Fe concentration, typical for small particles, covers the range 0.3–0.5, higher by an order of magnitude than in microspatter particles. The additional evidence is the presence of elements that compose the electrode rod (Cr, V, Ni and Cu) and the electrode coating (Ti, Al, Ca, P, S, Cr etc.) in the coarse particles.

For comparison, the last row of Table 2 contains data of the bulk fume composition at the current 14.3 A/mm² from Table 1, normalized in this way that the Fe concentration is accepted to be 40%; data for Na, Mg and O are taken from Ref. 20. Noteworthy, the composition of the coarse particles correlates fairly well with the results of the bulk analysis. It is consistent with the common assumption that the coarse particles dominate the bulk chemistry of welding fume, even if their number is relatively small.[6,20] In particular, this means that the bulk analysis is not relevant with respect to health aspects, since it gives information about the least respirable fume fraction.

## Individual particle analysis

On the individual particle level, the most important differences between the size fractions of welding fume particles were found with respect to their shape and the type of particle agglomeration. Tables 3–8 contain results of the cluster analysis of individual welding particles including relative abundance and average elemental weight concentrations for each particle group, separately for each size fraction. Since different mechanisms of formation are responsible for different chemical and morphological properties of the particles, a more detailed discussion is required for the fine (cut-off diameters 0.25 and 0.5 µm) and coarse (cut-off diameters > 1 µm) fractions, separately.

Figure 2 presents examples of the particles collected on stages 3, 4, and 5 accompanied by their molecular spectra. In the fine particle fractions, irregularly shaped species were most abundant. Such small particles represent highly agglomerated formations having typical spongy and fibrous structures formed by accumulation of primary nanometer-sized particles appearing due to condensation mechanism. Additionally, diameters of the particles collected on stages 3 and 4 (normally representing the fine particle fractions with an aerodynamic diameter up to 1 µm) were larger than the expected from the corresponding impactor stage cut-off size. This is explained by the non-compact structure of fine particles resulting in increase of the geometrical size compared to the aerodynamic one,[23] which determines the impactor stage classification.
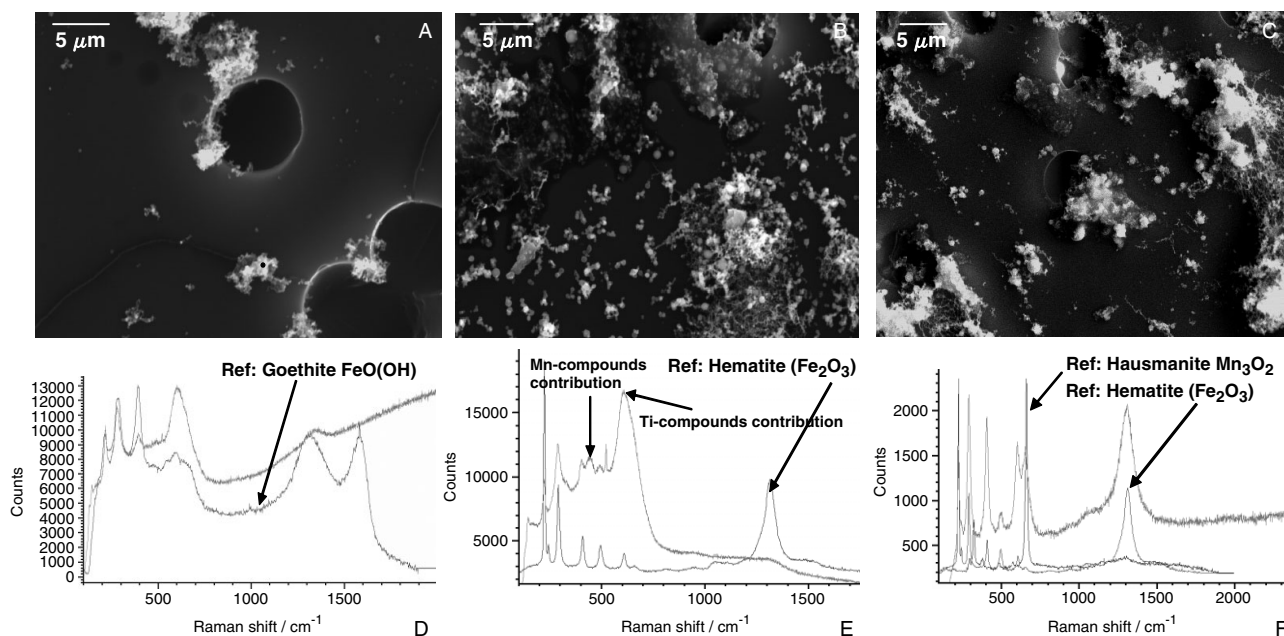


**Figure 2.** Visualisation of the welding particles' shape collected in A: stage 3 (cut-off 0.25 µm); B: stage 4 fraction (cut-off 0.5 µm), C: stage 5 (cut-off 1 µm); D, E, F: Examples of the molecular spectra of the typical individual welding particles from stages 3, 4, 5, respectively. Dark circular structures seen in panels A, C are the substrate pores.

**Table 3.** Elemental composition of the welding fume particles in the fraction 0.25–0.5 µm

| Group number | Group abundance % | Main group components, % | | | | | | | | | |
|---|---|---|---|---|---|---|---|---|---|---|---|
| | | Fe | Mn | Ca | K | Cl | Si | Mg | Na | O | C |
| 1 | 31 | 7.2 | 3.6 | 1.0 | 6.9 | — | 7.2 | 4.3 | 7.3 | 57 | 4.1 |
| 2 | 27 | 17 | 4.6 | — | 4.3 | — | 6.9 | 2.8 | 5.1 | 51 | 7.7 |
| 3 | 20 | 12 | 3.2 | — | 2.8 | — | 8.0 | 3.2 | 4.0 | 62 | 3.8 |
| 4 | 14 | 9.2 | 3.4 | 1.5 | 6.9 | 1.0 | 13 | 5.3 | 10 | 47 | 3.1 |
| 5 | 8 | 1.4 | — | — | 1.1 | 1.1 | 2.5 | — | 18 | 26 | 49 |

**Table 4.** Elemental composition of the welding fume particles in the fraction 0.5–1 µm

| Group number | Group abundance, % | Main group components, % | | | | | | | | |
|---|---|---|---|---|---|---|---|---|---|---|
| | | Fe | Mn | Ti | K | Si | Mg | Na | O | C |
| 1 | 43 | 18 | 3.3 | — | 2.6 | 5.1 | — | 1.7 | 63 | 4.9 |
| 2 | 41 | 8.8 | 2.4 | — | 3.4 | 5.0 | — | 1.4 | 73 | 4.4 |
| 3 | 10 | 22 | 1.5 | 1.5 | — | 19 | — | — | 48 | 7.3 |
| 4 | 5 | 37 | 6.4 | — | 4.2 | — | 1.6 | 2.0 | 47 | 1.4 |
| 5 | 1 | — | 4.0 | 5.0 | — | 13 | — | — | 33 | 45 |

**Table 5.** Elemental composition of the welding fume particles in the fraction 1–2 µm

| Group number | Group abundance, % | Main group components, % | | | | | | | | | | |
|---|---|---|---|---|---|---|---|---|---|---|---|---|
| | | Fe | Mn | Cr | Ti | K | D | Si | Al | Mg | Na | O | C |
| 1 | 39 | 31 | 5.5 | — | — | 2.7 | — | 7.5 | — | 1.4 | 1.3 | 40 | 8.4 |
| 2 | 25 | 44 | 4.4 | — | — | 1.7 | — | 4.4 | — | — | — | 38 | 4.8 |
| 3 | 18 | 54 | 3.2 | — | — | — | — | 3.0 | — | — | — | 33 | 4.2 |
| 4 | 17 | 17 | 6.1 | — | — | 5.1 | — | 11 | — | 1.8 | 2.5 | 44 | 8.6 |
| 5 | 1 | 2.0 | — | 2.2 | 3.2 | — | 1.2 | 2.2 | 3.2 | 6.0 | 1.0 | 9.3 | 69 |

**Table 6.** Elemental composition of the welding fume particles in the fraction 2–4 µm

| Group number | Group abundance, % | Main group components, % | | | | | | | | | | | |
|---|---|---|---|---|---|---|---|---|---|---|---|---|---|
| | | Fe | Mn | Ti | Ca | K | D | Si | Al | Mg | Na | O | N | C |
| 1 | 31 | 47 | 5.5 | 1.0 | — | 2.1 | — | 5.1 | — | 1.1 | — | 33 | — | 3.5 |
| 2 | 27 | 34 | 6.3 | 1.6 | — | 3.6 | — | 8.6 | — | 1.7 | 1.6 | 37 | — | 3.6 |
| 3 | 16 | 60 | 2.8 | — | — | — | — | 1.8 | — | — | — | 31 | — | 2.2 |
| 4 | 9 | 20 | 5.8 | 3.3 | 1.2 | 4.8 | 1.2 | 11 | 1.0 | 2.0 | 2.0 | 41 | 1.0 | 6.4 |
| 5 | 5 | 63 | 6.2 | — | — | 2.8 | — | 5.2 | — | — | — | 17 | — | 2.6 |
| 6 | 5 | 11 | — | 2.1 | 2.5 | — | — | 5.1 | 2.3 | 4.3 | — | 27 | — | 43 |
| 7 | 3 | 34 | 2.9 | 1.6 | 1.6 | 1.7 | — | 4.3 | 1.9 | 3.7 | — | 25 | — | 22 |
| 8 | 2 | 3.9 | — | 2.0 | 2.9 | — | — | 2.1 | 3.3 | 5.1 | — | 7.7 | — | 72 |
| 9 | 2 | 2.8 | — | — | 24 | — | 1.5 | 4.5 | 1.3 | 1.5 | 1.0 | 44 | 2.5 | 16 |

Observation of spongy structures in Fig. 2(A) and (B) stays in good agreement with known reports about fractal-like agglomerates of the nucleation mode particles.[7] A relatively high content of such agglomerates correlates with high concentration of Na and K in fine particles of condensation origin, which promotes their agglomeration due to adsorption of moisture.[10,13]

In compliance with the formation mechanism outlined above, the fine particles mainly contain low-boiling components of the electrode coating: ionizers and binders (Na and K silicates), gasifiers (magnesite, $MgCO_3$) and doping alloys (FeMn, FeSi) (Tables 4 and 5).

Inessential quantitative differences in elemental compositions were found while comparing groups (e.g. 1 with 4

**Table 7.** Elemental composition of the welding fume particles in the fraction 4–8 μm

| Group number | Group abundance, % | Main group components, % | | | | | | | | | | | | |
|---|---|---|---|---|---|---|---|---|---|---|---|---|---|---|
| | | Cu | Fe | Mn | Ti | Ca | K | Si | Al | Mg | Na | O | N | C |
| 1 | 24 | — | 56 | 5.0 | — | — | 1.2 | 3.3 | — | — | — | 29 | — | 2.9 |
| 2 | 23 | — | 46 | 6.1 | — | — | 2.1 | 5.7 | — | 1.1 | — | 33 | — | 2.8 |
| 3 | 21 | — | 37 | 5.5 | 1.0 | — | 3.0 | 8.0 | — | 1.9 | 1.1 | 36 | — | 5.9 |
| 4 | 14 | — | 21 | 6.1 | 9.5 | — | 5.9 | 8.7 | 1.9 | 2.0 | 2.1 | 38 | 1.7 | 2.8 |
| 5 | 7 | — | 67 | 8.9 | 1.1 | — | 2.5 | 3.0 | — | — | — | 13 | — | 2.8 |
| 6 | 5 | 2.6 | 6.2 | — | — | 7.4 | 1.5 | 13 | 6.3 | 1.7 | 2.2 | 38 | 1.6 | 19 |
| 7 | 4 | — | — | — | 1.5 | 1.9 | — | 2.2 | 3.6 | 4.7 | — | 11 | 5.6 | 68 |
| 8 | 2 | — | 1.1 | — | — | 35 | — | 2.4 | — | — | — | 45 | 2.7 | 11 |

**Table 8.** Elemental composition of the welding fume particles in the fraction > 8 μm

| Group number | Group abundance, % | Main group components, % | | | | | | | | | | | | |
|---|---|---|---|---|---|---|---|---|---|---|---|---|---|---|
| | | Fe | Mn | Cr | V | Ti | Ca | K | Si | Al | Mg | Na | O | N | C |
| 1 | 39 | 49 | 5.4 | — | — | — | — | 1.4 | 4.6 | — | — | — | 34 | — | 1.9 |
| 2 | 22 | 33 | 7.8 | — | — | 2.0 | — | 2.9 | 9.5 | — | 2.0 | 1.4 | 38 | — | 2.0 |
| 3 | 12 | 63 | 1.0 | — | — | — | — | — | — | — | — | — | 32 | — | 1.4 |
| 4 | 10 | 13 | 5.3 | — | 2.7 | 18 | 1.0 | 4.4 | 4.8 | 4.0 | 3.0 | 1.8 | 38 | 2.7 | 1.5 |
| 5 | 9 | 1.0 | — | 2.7 | — | — | 1.2 | — | 1.7 | 2.4 | 3.0 | — | 14 | 4.5 | 69 |
| 6 | 4 | 10 | — | — | 3.0 | 1.0 | 7.2 | 6.0 | 7.5 | 4.1 | 2.3 | — | 32 | 3.4 | 21 |
| 7 | 4 | 69 | 10 | — | — | 1.2 | — | 2.1 | 3.5 | — | — | — | 11 | — | 1.7 |

and 2 with 3) in Table 4. This may be caused by the temperature fluctuations followed by changing concentrations of vapours of individual elements and their compounds in the condensation zone.

The presence of sodium carbonates and silicates with high C-content is noteworthy in the fractions < 0.5 μm and 0.5–1 μm. In view of the high content of O, Mn is likely present at high oxidation state in these fractions, which is important because $MnO_2$ is the most toxic oxide of Mn.

It should also be mentioned that on stage 4 there are some agglomerates of small spherical particles in the typical chain forms (Fig. 2(B)). As it can be seen from Fig. 1(D) and (E), iron-containing compounds were only found in the forms of goethite and hematite. In the fraction of stage 5 (cut-off diameter 1 μm), spherical particles were suspended in a sort of webs of very fine particle chains (Fig. 2(C)). They represent probably the primary welding fume structures of nucleation mode particles, which can be considered as a result of inertial coagulation process.[23] Single spherical species were also observed quite frequently.

Figure 3 presents examples of particles from the coarse fractions (stage 6, 7, 8). The agglomerated structures contain fine particles deposited on the smooth surfaces of coarse particles. Since the fume particles collected on these stages are rich with Fe-containing phases with articulate magnetic properties, these types of formation seem to be caused by magnetic interaction between the particles. The compositions of the particles collected on stages 6 and 7 (cut-off diameters 2 and 4 μm, respectively) were very similar to each other and the most complex among all the particle fractions. The data gathered in Tables 5–8 lead to the conclusion that the larger the size of particles is, the wider is the range of elements they contain. The variety of elemental combinations also increases (the cluster analysis produces a larger number of partitions).

Owing to the microspatter mechanism of formation in coarse particle fractions, the elements are characterized by lower degrees of oxidation. Therefore, conditions for the emergence of very toxic Mn compounds in a highly oxidized state are not as favourable as in case of small particles.

The contribution of C compounds revealed by the low-Z EPMA is worth considering in detail. All the size fractions contain C-rich particles but their share is rather low (less than 9%)—e.g. group 5 in Tables 3–5 and 8, as well as groups 8 and 7 in Tables 6 and 7, respectively. The ratio of C and O in the fine C-rich particles confirms the suggested mechanism of their formation, which presumes that the fine particles contain small soot cores. For the fraction with < 0.5-μm-particle size, these cores may contribute noticeably to the whole particle composition, while for particles larger than 0.5 μm in diameter, the core plays only a minor role. Considering the coarse C-rich particles whose existence is clearly proven by EPMA (Tables 6–8, rows 8, 7 and 5, correspondingly), their formation cannot be explained by the same mechanism as for the case of the fine particles. Most probably, they appear as fragments of C-containing components of a coating layer. In this case, large fragments are more likely to be preserved in the course of the welding process, which explains the increase of the C-rich group population with the fraction size (Tables 5–8).
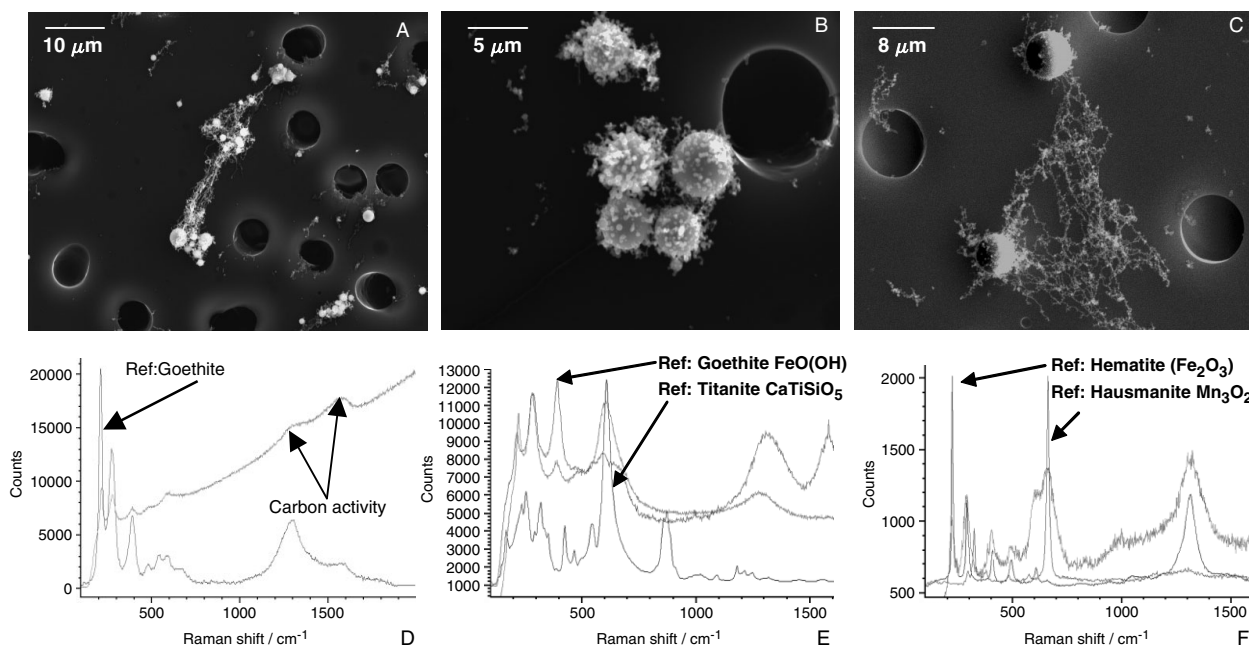
**Figure 3.** Visualisation of the welding particles' shape collected in A: stage 6 (cut-off 1 μm); B: stage 7 fraction (cut-off 4 μm), C: stage 8 (cut-off 8 μm); D, E, F: Examples of the molecular spectra of the typical individual welding particles from stages 6, 7, 8, respectively. Dark circular structures seen in panels A, B and C are the substrate pores.

The molecular spectra collected from the coarse particles (Fig. 3(D)–(F)) confirm these results. Moreover, the Raman activity of elemental C was detected together with goethite Raman shifts, while hematite was mostly agglomerated with hausmannite. No agglomerates of goethite and hausmannite were found in any of the particle fractions.

From the morphological point of view, Fig. 3(A) and (B) demonstrate significant differences in shape between particles from stages 6 and 7. The spherical particles captured on stage 6 have a smoother surface than those on stage 7. They do not show many inclusions, while agglomeration appeared in a limited degree. However, in some cases it was observed that the particles were connected to one another by a sort of chain structures. Similar structures were also observed on stages 5 and 8 (cut-off diameters 1 μm and 8 μm). In the case of the particles from stage 7 (e.g. Figure 3(B)), accumulation of spongy structures (typical for fine particles, Fig. 2(A)) on the surfaces of spherical ones is often observed. This way of agglomeration brings the idea of either adhesive or magnetic properties of both the covering and covered particles.

For particles from stage 8, this agglomeration was less intensive; however, large web-like structures of fine chains were rather abundant (see an example in Fig. 3(C)). Although the morphology of these structures seems to be similar to those occurring in stage 6 (Fig. 3(A)), their chemical compositions differ essentially, as can be seen from Fig. 3(D) and (F).

## CONCLUSION

Morphology and chemical composition of individual welding aerosol particles, depending on their size distribution, have been studied by applying a combination of micro- and trace analysis techniques. Strong correlations between the particles' elemental compositions and their size have been observed. In the fine fractions (0.25–0.5 μm), particles of irregular shapes are mainly rich in Fe, Si, Na and C. In the 0.5–2.0 μm fractions, the particles are spherical and their composition differs from the one observed for finer fraction: various types of Fe-rich particles (with and without Si content or with Mn content) are the most abundant. An increasing contribution of C-rich particles is observed in the size fraction above 2 μm. The MRS showed the presence of Fe-containing compounds, such as hematite and goethite, in all the size fractions. Evidences of some Fe oxyhydroxides containing Mn (also in the form of hausmannite) was found in the larger size fractions. The properties of fine and coarse welding fume particles revealed in these experiments correspond to the suggested mechanisms of their formation.

Interesting and probably far-reaching conclusions can be made in the context of the observed accumulation of fine fume particles on surfaces of the coarse ones or formation of large web-like structures. Referring to the effective trapping of welding particles, such agglomeration could be considered as a positive effect, since the particles become bigger and more irregularly shaped. Additionally, the smallest fraction tends to be immobilized by the larger one. These examples confirm the possibility of the welding aerosol evolution in which the most harmful species of welding fumes are concentrated in certain fractions with special dimensional and morphological parameters. These properties facilitate their removal from the fume and subsequently their neutralization. However, these statements are preliminary and require more fundamental study with respect to magnetic properties of the welding fumes.

## REFERENCES

1. Stern RM. *Arch. Environ. Health* 1983; **38**: 148.
2. Tandon RK, Ellis J, Crisp PT, Baker RS, Chenhall BE. *Welding J.* 1986; **65**: 231.
3. http://www.thefabricator.com/Safety/Safety Article.cfm? ID=851, accessed July 2005.
4. http://www.afscme.org/health/faq-weld.htm/#health%20haz, accessed July 2005.
5. Antonini JM. *Crit. Rev. Toxicol.* 2003; **33**: 61.
6. Jenkins NT, Pierce WM-G, Eagar TW. *Welding J.* 2005; **84**: 156.
7. Jenkins NT, Eagar TW. *Welding J.* 2005; **84**: 87.
8. Hewett P. *Am. Ind. Hyg. Assoc. J.* 1995; **56**: 128.
9. Jenkins NT. *Chemistry of Airborne Particles from Metallurgical Processing*, PhD dissertation. Massachusetts Institute of Technology: Cambridge, 2003.
10. Voitkevich VG. *Welding Fumes: Formation, Properties and Biological Effects*. Abington Publishing: Cambridge, 1995.
11. Oprya MV, Ennan AA, Mikhaylovskii SS. *1st International Scientific-Practical Conference ''Protection of Environment, Health and Safety in Welding''*. Astroprint: Odessa, 2002.
12. Zimmer AT, Biswas P. *J. Aerosol Sci.* 2001; **32**: 993.
13. Frolov VV (ed.). *Welding Process Theory*. Vysshaya Shkola: Moscow, 1998.
14. Willeke K, Baron PA (eds.). *Aerosol Measurement: Principles, Techniques and Applications*. Van Nostrand Reinhold: New York, 1993.
15. Ro C-U, Osán J, Van Grieken R. *Anal. Chem.* 1999; **71**: 1521.
16. Vekemans B, Janssens K, Vincze L, Adams F, Van Espen P. *X-Ray Spectrom.* 1994; **23**: 278.
17. Osán J, Szalóki I, Ro C-U, Van Grieken R. *Mikrochim. Acta* 2000; **132**: 349.
18. Szalóki I, Osán J, Ro C-U, Van Grieken R. *Spectrochim. Acta, Part B* 2000; **55**: 1017.
19. Bondarenko I, Treiger B, Van Malderen H, Van Grieken R, Van Espen P. *Spectrochim. Acta, Part B* 1996; **51**: 441.
20. Voitkevich VG, Bezruk LI, Yesaulenko GB. *Avtom. Svarka (Automated welding)* 1984; **6**(375): 33.
21. Yavdoshin IR, Pokhodnia IK. *1st International Scientific-Practical Conference ''Protection of Environment, Health and Safety in Welding''*. Astroprint: Odessa, 2002; 38.
22. Deam R, Bosworth M, Chen Z, French I, Haidar J, Lowke J, Norrish J, Tyagi V, Workman A. *Proceedings of the Technologic Developments and Advances for Australian Industry, International Welding and Joint Research Conference*. Welding Technology Institute of Australia: Silverwater, 1997.
23. Fuchs NA. *The Mechanics of Aerosols*. Pergamon: Oxford, 1964.